Usefulness of 3′-Deoxy-3′-^{18}F-Fluorothymidine PET for Predicting Early Response to Chemoradiotherapy in Head and Neck Cancer

Takehito Kishino[1], Hiroshi Hoshikawa[1], Yoshihiro Nishiyama[2], Yuka Yamamoto[2], and Nozomu Mori[1]

[1]*Department of Otolaryngology, Faculty of Medicine, Kagawa University, Kagawa, Japan; and* [2]*Department of Radiology, Faculty of Medicine, Kagawa University, Kagawa, Japan*

This study compared the utility of 3′-deoxy-3′-^{18}F-fluorothymidine PET (^{18}F-FLT PET) with that of ^{18}F-FDG PET for assessment of the early locoregional clinical outcomes of chemoradiotherapy for head and neck squamous cell carcinomas. **Methods:** From May 2006 to September 2010, 28 patients with head and neck squamous cell carcinomas underwent ^{18}F-FLT and ^{18}F-FDG PET before radiation therapy (RT), 4 wk after the initiation of RT, and 5 wk after completion of RT. PET images were evaluated qualitatively for regions of focally increased metabolism and were analyzed in relation to residual accumulation and local disease control. **Results:** During RT, ^{18}F-FLT uptake decreased more significantly than ^{18}F-FDG uptake. ^{18}F-FLT accumulations disappeared in 34 of 54 lesions (63%), and negative predictive value was 97%. ^{18}F-FDG PET during RT also had a high negative predictive value (100%), but only 9 lesions (16%) showed complete absence of accumulation. The specificity and overall accuracy of ^{18}F-FLT PET were significantly higher than those of ^{18}F-FDG PET both during and after RT. In particular, high significance was attributable to the results of the evaluations of primary lesions. There were significant differences in 3-y local control between the residual-accumulation and no-accumulation groups on both posttreatment ^{18}F-FLT PET ($P < 0.0001$) and posttreatment ^{18}F-FDG PET ($P = 0.0081$). **Conclusion:** ^{18}F-FLT PET during RT and early follow-up facilitates the selection of optimal further therapy and the prediction of outcomes.

Key Words: FLT PET; FDG PET; chemoradiotherapy; head and neck; early evaluation

J Nucl Med 2012; 53:1521–1527
DOI: 10.2967/jnumed.111.099200

Radiation therapy (RT) plays an important role in the management of locally advanced head and neck squamous cell carcinomas (HNSCCs). To preserve organ function, concurrent chemoradiotherapy is now widely applied as the definitive treatment for locoregionally advanced HNSCCs (*1*). If persistent or recurrent tumors can be detected accurately, salvage surgery may be offered.

The current method for assessing the response of a solid tumor to RT is assessment of tumor size change by anatomic imaging modalities (*2*). However, the size of a tumor after treatment is not directly related to the viability of tumor cells because morphologic changes can include scarring due to either therapy or inflammation. Thus, these imaging techniques have limitations for assessing therapeutic effects.

Several studies have suggested that ^{18}F-FDG PET might be useful for assessment of therapeutic responses (*3–6*). However, ^{18}F-FDG is also metabolized at sites of inflammation and in other reactive states, so that false-positive results may be obtained because of inflammatory changes remaining within the first few posttreatment months.

Recently, a thymidine analog, 3′-deoxy-3′-^{18}F-fluorothymidine (^{18}F-FLT), was introduced as a stable cell proliferation imaging agent (*7*). This tracer is trapped within the cytosol after being monophosphorylated by thymidine kinase-1, a principal enzyme in the salvage pathway of DNA synthesis (*8*). ^{18}F-FLT accumulation is dependent on the presence of thymidine kinase-1, which is closely associated with cellular proliferation (*8*). ^{18}F-FLT has thus been found to be useful for noninvasive assessment of the proliferation rates of several types of cancer, including HNSCC (*9–11*). Moreover, ^{18}F-FLT PET has been used for early response monitoring of chemotherapy and RT (*12–14*). Yue et al. (*15*) examined esophageal squamous cell cancer patients during RT and reported an almost complete absence of tumor proliferation after 30 Gy of irradiation and a complete absence after 40 Gy of irradiation. Recently, Troost et al. (*16*) studied oropharyngeal cancer patients before RT and then 2 and 4 wk after the initiation of RT. In primary lesions, the relative decrease in maximal standardized uptake value (SUV) was 55% when pretreatment and second scans were compared and there was a 34% difference between the second and third scans. As to lymph node metastases, similar patterns were observed. However, there are few studies comparing the accuracy of ^{18}F-FLT PET and ^{18}F-FDG PET in HNSCC at an early stage after RT.

Received Nov. 14, 2011; revision accepted May 2, 2012.
For correspondence or reprints contact: Hiroshi Hoshikawa, Department of Otolaryngology, Faculty of Medicine, Kagawa University, 1750-1, Ikenobe, Miki-cho, Kita-gun, Kagawa, Japan.
E-mail: hiro@med.kagawa-u.ac.jp
Published online Jul. 7, 2012.

In this study, patients with HNSCC underwent 3 consecutive ^{18}F-FLT PET and ^{18}F-FDG PET scans: once before, once during, and finally a few weeks after completion of RT. The aims of this study were to monitor early tumor responses based on visual inspection and to compare the accuracy of ^{18}F-FLT PET and ^{18}F-FDG PET in patients with HNSCC.

MATERIALS AND METHODS

Patients

From May 2006 to September 2010, 28 patients with newly diagnosed HNSCCs treated with concurrent chemoradiotherapy were studied. All tumors were staged according to the 2002 International Union Against Cancer TNM staging system (*17*). All 28 primary lesions were histopathologically confirmed. A total of 30 lesions of cervical lymph node involvement were radiologically assessed before RT. The study was approved by the local ethics committee, and written informed consent was obtained from all patients.

Treatment and Follow-up

RT was administered to primary and neck regions once a day using 4-MV photons with a pair of bilaterally opposed fields for the upper neck and an anterior port for the lower neck. Patients were irradiated with a total dose of 60–70 Gy in once-daily fractions of 2 Gy. After 40 Gy had been administered, the clinical target volume was reduced to encompass only the primary region and the involved neck nodes. Twenty-two patients received chemotherapy, which consisted of 1–2 courses of systemic chemotherapy. Five patients received chemotherapy with cisplatin (70 mg/m^2) and 5-fluorouracil (1,000 mg/m^2 continuous infusion for 5 d), and the other 17 patients underwent chemotherapy with nedaplatin (80 mg/m^2) and S-1 (a novel oral anticancer drug consisting of a mixture of 1 M tegafur, 0.4 M 5-chloro-2,4-dehydroxypyrimidine, and 1 M potassium oxonate), administered orally twice a day for 14 d at the following doses on the basis of body surface area: $<$1.5 m^2, 80 mg/d; $\geq$1.5 m^2, 100 mg/d. Nedaplatin is a platinum derivative that was developed as a less nephrotoxic agent than cisplatin. Nedaplatin has been reported to be at least as effective as cisplatin for HNSCC (*18,19*). In S-1, tegafur is a prodrug of 5-fluorouracil, 5-chloro-2,4-dehydroxypyrimidine enhances the serum 5-fluorouracil concentrations, and potassium oxonate reduces adverse reactions in the digestive tract (*20*). Five patients with T2 laryngeal cancer and one with decreased renal function received weekly docetaxel (10 mg/m^2) chemotherapy 4–6 times concomitantly with RT.

Patients were followed up every 1–2 mo for the first 2 y after RT and then every 3 mo. A physical examination including endoscopy was performed at each follow-up session. The assessments included repeated CT scans or MRI every 3–6 mo.

Responses to chemoradiotherapy were clinically evaluated on the basis of endoscopic, radiographic, and pathologic findings. When a residual or recurrent tumor was suspected in the primary region, biopsy was performed under local or general anesthesia.

Patients with positive CT or PET findings in lymph nodes were considered to have indications for the performance of neck dissection. Four patients were diagnosed as having persistent or recurrent disease in lymph nodes, and 5 lymph nodes were confirmed to have tumor involvement (3 patients had 1 metastatic lymph node, and 1 patient had 2 metastatic lymph nodes).

^{18}F-FLT Synthesis

^{18}F-FLT was synthesized using the method described by Machulla et al. (*21*) with a radiochemical purity of more than 95%.

PET Acquisition

Integrated PET and CT images were acquired using either dedicated PET and CT systems (19 patients) or a hybrid PET/CT system (9 patients). Patients were instructed to fast for at least 5 h before ^{18}F-FLT and ^{18}F-FDG PET examinations, although oral hydration with glucose-free water was allowed. For ^{18}F-FDG PET, a normal peripheral blood glucose level was confirmed. Dedicated PET images were acquired using an ECAT EXACT HR+ scanner (Siemens/CTI). The imaging system allowed simultaneous acquisition of 63 transverse PET images per field of view, for a total axial field of view of 15.5 cm. PET scans were acquired 60 min after intravenous injection of ^{18}F-FLT (3.5 MBq/kg) or ^{18}F-FDG (3.5 MBq/kg), with 2 or 3 min per bed position in 3-dimensional mode. Transmission scans were obtained using a ^{68}Ge rod source for the purpose of attenuation correction. PET images were reconstructed with ordered-subset expectation maximization using 2 iterations and 8 subsets. Starting in April of 2010, hybrid PET/CT acquisitions were performed with an integrated PET/CT system (Biograph mCT; Siemens Medical Solutions). Emission images were obtained 60 min after intravenous injection of ^{18}F-FLT (3.5 MBq/kg) or 120 min after intravenous injection of ^{18}F-FDG (3.5 MBq/kg) (2 min per bed position; scan length, 21.6 cm per bed position) from the neck to the pelvis (5–7 bed positions) and coregistered with an unenhanced CT scan of the same region (120 kV; quality reference mAs, 210 mAs [using CARE Dose4D; Siemens]; reconstructed slice thickness, 5 mm). The mean intervals between scans before RT, during RT and after RT, for both ^{18}F-FLT PET and ^{18}F-FDG PET, were 4, 2, and 2 d, respectively.

PET Image Analysis

PET images were reviewed on a Sun Microsystems workstation (Siemens/CTI) in transverse, coronal, and sagittal planes along with maximum-intensity-projection images. ^{18}F-FLT and ^{18}F-FDG PET images were read at random, with an interval of several days between interpretations. The observers were masked to all identifying information. Any differences in opinion were resolved by reaching a consensus. The PET images were evaluated qualitatively for regions of focally increased metabolism. Increased uptake to a level appreciably greater than that in the surrounding tissue was considered to indicate malignancy.

A finding was considered true-positive if a tumor was histopathologically proven at follow-up in an area with residual uptake. A finding was considered true-negative if no residual accumulation was shown and no tumor recurrence was found at follow-up. A finding was considered false-positive if it was not recurrent at follow-up in an area with residual uptake. A finding was considered false-negative if a tumor was histopathologically proven or the finding was recurrent at follow-up in an area with no uptake.

Data Analysis

Statistical analyses were performed using the Wilcoxon signed-rank test and the Mann–Whitney *U* test. Actual local control was estimated by the Kaplan–Meier method. Hazard ratios with 95% confidence intervals were calculated, with a *P* value of less than 0.05 considered to be statistically significant.

RESULTS

Patient and Tumor Characteristics

Patient and tumor characteristics are summarized in Table 1. In all patients with primary lesions of HNSCC, focally increased ^{18}F-FLT and ^{18}F-FDG uptake was visible. As to metastatic lymph nodes, only 1 metastatic node could not be detected by ^{18}F-FLT PET, although ^{18}F-FDG PET and CT yielded a positive diagnosis.

The first PET scans were acquired within 3 wk before the start of RT. The second scans were acquired at the approximately 40-Gy point during RT (median, 42 Gy; range, 30–52 Gy, and median, 5 wk; range, 3–7 wk after the start of RT). The third scans were acquired after the completion of RT (median, 5 wk; range, 3–11 wk). Some of the second PET scans could not be obtained because of scheduling errors (^{18}F-FLT PET in 2 patients and ^{18}F-FDG PET in 1 patient). Some of the third ^{18}F-FDG PET scans could not be obtained because of the condition of the patient (2 patients). The median follow-up time of surviving patients from the beginning of treatment was 39 mo (range, 12–65 mo). During the follow-up period, 4 primary sites and 5 lymph nodes showed residual or recurrent disease. At the last follow-up, 24 patients were alive and 4 had died. All deaths were tumor-related.

Changes in ^{18}F-FLT and ^{18}F-FDG Uptake with Irradiation

Figure 1 shows a typical case of hypopharyngeal cancer. The ^{18}F-FLT accumulations in primary and metastatic lesions showed apparent decreases during RT, whereas ^{18}F-FDG accumulations persisted.

In the second ^{18}F-FLT scan, 34 of 54 lesions (63%) demonstrated the absence of ^{18}F-FLT accumulation whereas ^{18}F-FDG accumulation disappeared in only 9 of 56 lesions (16%) during RT ($P < 0.0001$). The absence of ^{18}F-FLT accumulation after RT slightly increased to 69% (40/58), and the absence of ^{18}F-FDG accumulation after RT significantly increased to 40% during RT (21/53) ($P = 0.0018$). Although no significant difference was observed between primary lesions and lymph node metastases during treatment on ^{18}F-FLT PET scans, the absence of ^{18}F-FLT accumulation was significantly more common in the primary lesions than in lymph node metastases after treatment ($P < 0.05$). In contrast, the rate of disappearance of ^{18}F-FDG accumulation on

TABLE 1
Patient Characteristics

Patient no.	Site	Sex	Age (y)	Clinical stage	During RT (Gy)		After RT (wk)	
					^{18}F-FLT PET2	^{18}F-FDG PET2	^{18}F-FLT PET3	^{18}F-FDG PET3
1	Oropharynx	M	78	T2N0M0	40	40	4	5
2	Oropharynx	M	83	T2N0M0	30	30	4	4
3	Oropharynx	M	63	T2N1M0	44	44	5	5
4	Oropharynx	M	73	T2N2bM0	38	38	5	NA
5	Oropharynx	M	58	T2N2bM0	32	32	5	5
6	Oropharynx	M	67	T3N1M0	NA	42	7	7
7	Oropharynx	F	71	T3N1M0	48	48	6	6
8	Oropharynx	M	50	T3N2aM0	44	44	4	5
9	Oropharynx	M	57	T4bN2cM0	NA	NA	5	5
10	Hypopharynx	M	69	T1N1M0	38	38	6	6
11	Hypopharynx	M	78	T2N0M0	40	40	4	5
12	Hypopharynx	M	63	T2N1M0	48	48	4	5
13	Hypopharynx	M	40	T2N2bM0	44	44	7	4
14	Hypopharynx	M	65	T2N2aM0	30	30	4	4
15	Hypopharynx	M	56	T2N2bM0	44	44	4	4
16	Hypopharynx	M	74	T2N2bM1	40.5	40.5	6	5
17	Hypopharynx	M	64	T3N2bM0	40	40	4	4
18	Hypopharynx	M	57	T4aN2cM0	42	42	3	4
19	Larynx	M	69	T2N0M0	50	50	6	11
20	Larynx	M	53	T2N0M0	50	52	4	4
21	Larynx	M	71	T2N0M0	46	46	4	4
22	Larynx	M	76	T2N1M0	44	44	5	5
23	Larynx	M	73	T2N2bM0	38	38	5	NA
24	Larynx	M	73	T3N0M0	42	42	5	5
25	Larynx	M	63	T3N1M0	40	40	4	4
26	Larynx	M	82	T3N1M0	40	42	4	4
27	Maxillary sinus	F	68	T4aN1M0	44	44	5	5
28	Oral cavity	F	83	T2N2bM0	42	42	7	4

NA = not available; PET2 = second PET scan; PET3 = third PET scan.

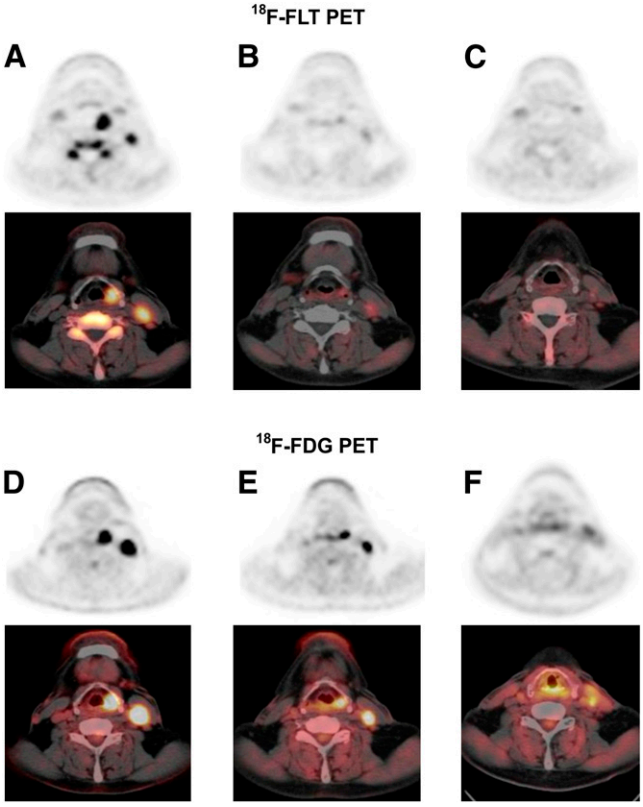

FIGURE 1. PET images of patient with hypopharyngeal cancer (patient 14, Table 1) before RT (A and D), 3 wk after initiation of RT (B and E), and 4 wk after end of RT (C and F). Pretreatment ^{18}F-FLT and ^{18}F-FDG axial PET images showed increased metabolism in primary tumor and metastatic lymph node (^{18}F-FLT SUVs, 9.16 and 6.06, respectively; ^{18}F-FDG SUVs, 21.81 and 13.37, respectively). ^{18}F-FLT and ^{18}F-FDG SUVs decreased after 30 Gy of irradiation (^{18}F-FLT SUVs, 2.86 and 2.14, respectively, and ^{18}F-FDG SUVs, 11.44 and 6.39, respectively). ^{18}F-FLT uptake in primary site and lymph nodes was same as in surrounding muscle (SUVs of 0.93, 0.9, and 0.9, respectively) at 4 wk after completion of treatment, whereas increased uptake of ^{18}F-FDG persisted (SUV of 4.66 in primary lesion and 3.75 in lymph node). Patient was alive and without evidence of recurrent disease 19 mo after therapy.

^{18}F-FDG PET was significantly higher in lymph node metastases than in primary lesions both during and after treatment ($P < 0.05$) (Fig. 2).

Correlation Between Signal Change on PET and Local Control

The results of qualitative assessments are presented in Tables 2 and 3. During midtreatment imaging, ^{18}F-FDG PET had high sensitivity (100%) and a high negative predictive value (100%) but low specificity (19%), a low positive predictive value (PPV) (17%), and low overall accuracy (30%). In contrast, midtreatment ^{18}F-FLT PET showed significantly higher specificity (72%) and overall accuracy (74%) than ^{18}F-FDG PET ($P < 0.0001$ and $P < 0.0001$, respectively). Only 1 primary lesion, in patient 9, showed a false-negative result with ^{18}F-FLT PET both during and after RT. Compared with the results obtained during RT, the specificity and overall accuracy of posttreatment ^{18}F-FDG PET were significantly improved ($P = 0.003$ and $P = 0.007$, respectively). Although all parameters on posttreatment ^{18}F-FLT PET tended to improve in comparison to those during RT, the differences did not reach statistical significance. Specificity and overall accuracy for lymph node metastases with ^{18}F-FLT PET were the same as those with ^{18}F-FDG PET at 5 wk after RT.

All lesions were divided into 2 groups: residual accumulation and no accumulation. The Kaplan–Meier method was used to identify significant differences in 3-y local control between the 2 groups based on posttreatment ^{18}F-FLT PET (hazard ratio, 25.57; 95% confidence interval, 5.739–113.9; $P < 0.0001$) and posttreatment ^{18}F-FDG PET (hazard ratio, 6.062; 95% confidence interval, 1.597–23.02; $P = 0.0081$). No significant differences were detected between ^{18}F-FLT PET and ^{18}F-FDG PET during treatment (Fig. 3).

DISCUSSION

^{18}F-FLT retention has been shown to correlate with thymidine uptake and thymidine kinase-1 activity (*8,22*). Thymidine kinase-1 activity is extremely sensitive to ionizing radiation, and changes in ^{18}F-FLT uptake are thought to reflect the direct biologic effect of RT (*23,24*). Yang et al. (*25*) showed ^{18}F-FLT uptake by SCCVII tumor cells to be significantly reduced within 24 h after a single dose of irradiation, with no visible tumor shrinkage or morphologic change. In addition, the tumor uptake of ^{18}F-FDG did not decrease 24 h after radiation, at a time when there was a significant reduction in ^{18}F-FLT tumor uptake. They concluded that reduced ^{18}F-FLT SUV preceded reduced ^{18}F-FDG uptake, suggesting that decreased cell proliferation precedes changes in glucose metabolism.

In experimental models of esophageal carcinoma (*26*), ^{18}F-FLT uptake after docetaxel plus irradiation declined by 75% compared with baseline by 2 d after chemoradiotherapy, whereas the decrease in ^{18}F-FDG uptake was gradual and less pronounced.

In clinical practice, Herrmann et al. (*12*) found that ^{18}F-FLT maximal SUV had already decreased significantly 2 d after the chemotherapy in non-Hodgkin lymphoma patients. Furthermore, the authors were able to detect a significant difference in the reduction of tumoral ^{18}F-FLT uptake between patients reaching a partial response and patients reaching a complete response at the end of therapy. Kenny et al. (*13*) examined breast cancer patients before and 1 wk after neoadjuvant chemotherapy and found that the decrease in ^{18}F-FLT SUV was significantly different between patients with clinical responses and patients with stable disease.

In head and neck cancer patients, Menda et al. (*27*) demonstrated a significant decrease in ^{18}F-FLT uptake after 10 Gy of RT for HNSCCs. Troost et al. (*16*) examined oropharyngeal cancer patients before treatment and 2 and 4 wk after initiation of RT. The reduction in SUVs was more than 2-fold in the initial phase of treatment and a further 2-fold in the fourth week. They concluded that defining the tumor subvolume with ^{18}F-FLT PET and dose escalation to these

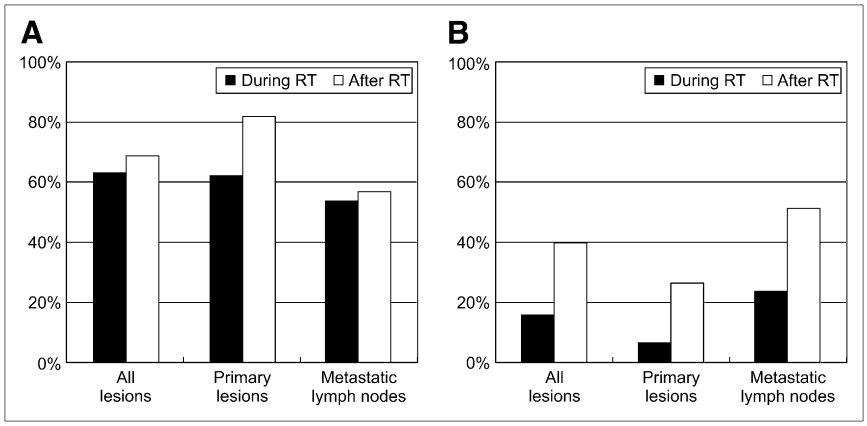

FIGURE 2. Rates at which accumulation of ^{18}F-FLT (A) and ^{18}F-FDG (B) disappeared during and after RT. In both primary lesions and lymph node metastases, rate during RT was significantly higher for ^{18}F-FLT than for ^{18}F-FDG ($P < 0.001$ and $P < 0.01$, respectively). After RT, no significant difference was found in lymph node metastases, whereas primary lesions differed significantly between ^{18}F-FLT PET and ^{18}F-FDG PET ($P < 0.001$).

regions was feasible. On the basis of these findings, ^{18}F-FLT PET is expected to assess the therapeutic response much earlier than currently used imaging modalities, including ^{18}F-FDG PET.

However, few studies have examined whether changes in ^{18}F-FLT PET correlate clinically with local control or survival. Only 1 report showed a correlation between ^{18}F-FLT uptake and survival in head and neck tumor patients (*28*). The authors reported a significant correlation between pretreatment ^{18}F-FLT SUVs and survival. However, their study had a small sample size (19 malignant and 1 benign tumor) and a short follow-up time (median, 18 mo).

The optimal timing of posttreatment ^{18}F-FDG PET after chemoradiotherapy has yet to be defined. In general, the rate of false-positive cases declines with the interval between the end of therapy and PET. Several authors have suggested 10–12 wk after the end of treatment (*29–32*), but others showed that negative PET findings accurately determined a complete response to therapy within 8 wk (*33–35*). Previously, we examined the usefulness of early posttreatment ^{18}F-FDG PET for assessing local control quantitatively and qualitatively (*36*). We found the combined analysis of posttreatment SUV and percentage change in SUV to be useful for predicting the therapeutic responses of metastatic lymph nodes. However, we still have the problem of how to handle the positive findings of both qualitative and quantitative analyses involving the primary site.

In the present study, to compare the utility of ^{18}F-FLT PET with that of ^{18}F-FDG PET for assessment of the early locoregional clinical outcomes of chemoradiotherapy for patients with HNSCCs, we performed ^{18}F-FLT and ^{18}F-FDG PET before RT, 4 wk after the initiation of RT, and 5 wk after completion of RT. We observed that ^{18}F-FLT uptake was significantly decreased compared with that of ^{18}F-FDG during and after RT. ^{18}F-FLT accumulations during RT disappeared in 34 of 54 lesions (63%), and negative predictive value was 97%. ^{18}F-FDG PET during RT also had a high negative predictive value (100%), but only 9 lesions showed absence of ^{18}F-FDG. ^{18}F-FLT PET yielded 1 false-negative result during and after RT. This patient had advanced oropharyngeal cancer, and progressive necrosis occurred during and after chemoradiotherapy. Although residual cancer cells were not detected by excisional biopsy, tumor persistence was suspected from clinical findings. In this case, a remarkable blood flow reduction due to necrosis might have accounted for the absence of ^{18}F-FLT accumulation.

The appropriate timing of intratherapy PET scans is important. Everitt et al. (*37*) assessed patients with non–small cell lung cancer undergoing chemoradiotherapy. Arrest of tumor cell proliferation became apparent after 20 Gy in 2 patients. The authors suggested that measurement of

TABLE 2
Comparison of Qualitative (Visual) Analysis of PET During RT

Parameter	Tracer	Sensitivity	Specificity	PPV	NPV	Accuracy
All lesions	^{18}F-FLT PET	87.5% (7/8)	72%* (33/46)	35% (7/20)	97% (33/34)	74%* (40/54)
	^{18}F-FDG PET	100% (8/8)	19% (9/48)	17% (8/47)	100% (9/9)	30% (17/56)
Primary lesions	^{18}F-FLT PET	67% (2/3)	65%* (15/23)	20% (2/10)	94% (15/16)	65%† (17/26)
	^{18}F-FDG PET	100% (3/3)	8% (2/24)	12% (3/25)	100% (2/2)	19% (5/27)
Metastatic LNs	^{18}F-FLT PET	100% (5/5)	65%† (15/23)	38% (5/13)	100% (15/15)	71%‡ (20/28)
	^{18}F-FDG PET	100% (5/5)	29% (7/24)	23% (5/22)	100% (7/7)	41% (12/29)

*$P < 0.001$ when compared with ^{18}F-FDG PET.
†$P < 0.01$ when compared with ^{18}F-FDG PET.
‡$P < 0.05$ when compared with ^{18}F-FDG PET.
PPV = positive predictive value; NPV = negative predictive value; LNs = lymph nodes.

TABLE 3
Comparison of Qualitative (Visual) Analysis of PET After RT

Parameter	Tracer	Sensitivity	Specificity	PPV	NPV	Accuracy
All lesions	^{18}F-FLT PET	89% (8/9)	80%* (39/49)	44% (8/18)	98% (39/40)	81%* (47/58)
	^{18}F-FDG PET	100% (9/9)	48% (21/44)	28% (9/32)	100% (21/21)	57% (30/53)
Primary lesions	^{18}F-FLT PET	75% (3/4)	92%† (22/24)	60% (3/5)	96% (22/23)	89%† (25/28)
	^{18}F-FDG PET	100% (4/4)	32% (7/22)	21% (4/19)	100% (7/7)	42% (11/26)
Metastatic LNs	^{18}F-FLT PET	100% (5/5)	68% (17/25)	38% (5/13)	100% (17/17)	73% (22/30)
	^{18}F-FDG PET	100% (5/5)	64% (14/22)	38% (5/13)	100% (14/14)	70% (19/27)

*$P < 0.01$ when compared with ^{18}F-FDG PET.
†$P < 0.001$ when compared with ^{18}F-FDG PET.
PPV = positive predictive value; NPV = negative predictive value; LNs = lymph nodes.

^{18}F-FLT uptake in tumors after 40 Gy might possibly be used to determine whether accelerating RT administration to counteract accelerated proliferation was warranted.

In the present study, the disappearance of ^{18}F-FLT accumulation was significantly more common in the primary lesions (from 62% to 82%) than in lymph node metastases (from 54% to 57%) 5 wk after RT. In addition, the specificity and overall accuracy of posttreatment ^{18}F-FLT PET in the primary site was significantly higher than that of ^{18}F-FDG PET ($P < 0.001$).

Our previous data (*36*) revealed that ^{18}F-FDG PET was useful for predicting the therapeutic responses of metastatic lymph nodes 5 wk after the irradiation. In this study, the accuracy of ^{18}F-FDG PET was the same as that of ^{18}F-FLT PET in metastatic lymph nodes after the therapy. These results suggest that ^{18}F-FLT PET was more useful for assessing early locoregional clinical outcomes in primary lesions and that ^{18}F-FLT PET may discriminate tumors from posttreatment inflammation more effectively than ^{18}F-FDG PET.

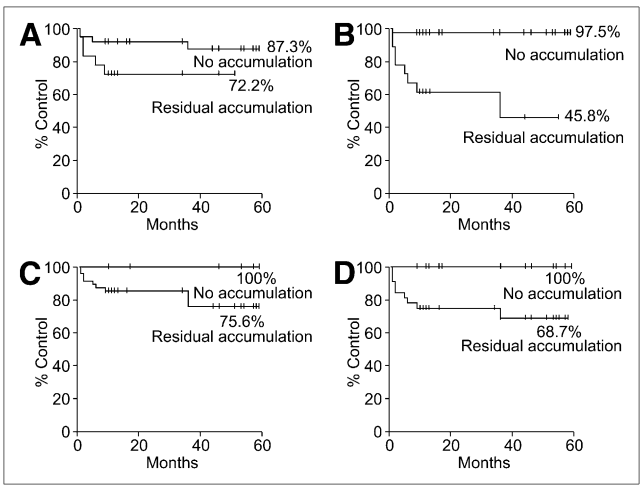

FIGURE 3. Local control in residual-accumulation and no-accumulation groups. Kaplan–Meier estimates are shown for local control on ^{18}F-FLT PET during treatment (A), on ^{18}F-FLT PET after treatment (B), on ^{18}F-FDG PET during treatment (C), and on ^{18}F-FDG PET after treatment (D). Differences in local control between 2 groups on posttreatment ^{18}F-FLT PET (97.5% vs. 45.8%, $P < 0.0001$) and posttreatment ^{18}F-FDG PET (100% vs. 68.7%, $P = 0.0081$) were significant.

For the analysis of ^{18}F-FDG uptake in the pathologic target volume, various approaches have been proposed. Semiquantitative analyses using maximal SUV are widely applied to assess the efficacy of treatments in various types of cancer. In the present study, we tried to predict early therapeutic responses with maximal SUV. However, no significant differences were found between the no-recurrence group and the recurrence group in the ^{18}F-FLT and ^{18}F-FDG PET study. Other semiquantitative analyses (e.g., change in SUV and tumor–to–normal-tissue ratio) or quantitative analysis (e.g., metabolic response) may make it challenging to understand the relationship between tracer uptake and tumor properties.

Our study population was heterogeneous with respect to tumor entities. Patient numbers were too small to allow analysis of the results by primary site location. Therefore, larger-population studies are needed to confirm the validity of these findings.

CONCLUSION

Concurrent chemoradiotherapy is widely used as the definitive treatment for advanced HNSCCs. ^{18}F-FLT PET during treatment and early follow-up has the potential to predict therapeutic responses and identify patients needing close follow-up to detect persistent or recurrent disease. ^{18}F-FLT PET assessment of therapeutic responses has potential for determining the optimal treatment course and predicting outcome.

DISCLOSURE STATEMENT

The costs of publication of this article were defrayed in part by the payment of page charges. Therefore, and solely to indicate this fact, this article is hereby marked "advertisement" in accordance with 18 USC section 1734.

ACKNOWLEDGMENT

No potential conflict of interest relevant to this article was reported.

REFERENCES

1. Bourhis J, Eschwege F. Radiotherapy-chemotherapy combinations in head and neck squamous cell carcinoma: overview of randomized trials. *Anticancer Res.* 1996;16:2397–2402.
2. Therasse P, Arbuck SG, Eisenhauer EA, et al. New guidelines to evaluate the response to treatment in solid tumors. European Organization for Research and Treatment of Cancer, National Cancer Institute of the United States, National Cancer Institute of Canada. *J Natl Cancer Inst.* 2000;92:205–216.
3. Kitagawa Y, Sano K, Nishizawa S, et al. FDG-PET for prediction of tumour aggressiveness and response to intra-arterial chemotherapy and radiotherapy in head and neck cancer. *Eur J Nucl Med Mol Imaging.* 2003;30:63–71.
4. McCollum AD, Burrell SC, Haddad RI, et al. Positron emission tomography with ^{18}F-fluorodeoxyglucose to predict pathologic response after induction chemotherapy and definitive chemoradiotherapy in head and neck cancer. *Head Neck.* 2004;26:890–896.
5. Isles MG, McConkey C, Mehanna HM. A systematic review and meta-analysis of the role of positron emission tomography in the follow up of head and neck squamous cell carcinoma following radiotherapy or chemoradiotherapy. *Clin Otolaryngol.* 2008;33:210–222.
6. Ware RE, Matthews JP, Hicks RJ, et al. Usefulness of fluorine-18 fluorodeoxyglucose positron emission tomography in patients with a residual structural abnormality after definitive treatment for squamous cell carcinoma of the head and neck. *Head Neck.* 2004;26:1008–1017.
7. Shields AF, Larson SM, Grunbaum Z, Graham MM. Short-term thymidine uptake in normal and neoplastic tissues: studies for PET. *J Nucl Med.* 1984;25:759–764.
8. Rasey JS, Grierson JR, Wiens LW, Kolb PD, Schwartz JL. Validation of FLT uptake as a measure of thymidine kinase-1 activity in A549 carcinoma cells. *J Nucl Med.* 2002;43:1210–1217.
9. Francis DL, Freeman A, Visvikis D, et al. In vivo imaging of cellular proliferation in colorectal cancer using positron emission tomography. *Gut.* 2003; 52:1602–1606.
10. van Westreenen HL, Cobben DC, Jager PL, et al. Comparison of ^{18}F-FLT PET and ^{18}F-FDG PET in esophageal cancer. *J Nucl Med.* 2005;46:400–404.
11. Yamamoto Y, Nishiyama Y, Ishikawa S, et al. Correlation of ^{18}F-FLT and ^{18}F-FDG uptake on PET with Ki-67 immunohistochemistry in non-small cell lung cancer. *Eur J Nucl Med Mol Imaging.* 2007;34:1610–1616.
12. Herrmann K, Wieder HA, Buck AK, et al. Early response assessment using 3′-deoxy-3′-[^{18}F]fluorothymidine-positron emission tomography in high-grade non-Hodgkin's lymphoma. *Clin Cancer Res.* 2007;13:3552–3558.
13. Kenny L, Coombes RC, Vigushin DM, Al-Nahhas A, Shousha S, Aboagye EO. Imaging early changes in proliferation at 1 week post chemotherapy: a pilot study in breast cancer patients with 3′-deoxy-3′-[^{18}F]fluorothymidine positron emission tomography. *Eur J Nucl Med Mol Imaging.* 2007;34:1339–1347.
14. Pio BS, Park CK, Pietras R, et al. Usefulness of 3′-[F-18]fluoro-3′-deoxythymidine with positron emission tomography in predicting breast cancer response to therapy. *Mol Imaging Biol.* 2006;8:36–42.
15. Yue J, Chen L, Cabrera AR, et al. Measuring tumor cell proliferation with ^{18}F-FLT PET during radiotherapy of esophageal squamous cell carcinoma: a pilot clinical study. *J Nucl Med.* 2010;51:528–534.
16. Troost EG, Bussink J, Hoffmann AL, Boerman OC, Oyen WJ, Kaanders JH. ^{18}F-FLT PET/CT for early response monitoring and dose escalation in oropharyngeal tumors. *J Nucl Med.* 2010;51:866–874.
17. Sobin LH, Wittecind C. *TNM Classification of Malignant Tumors.* 6th ed. New York, NY: Wiley-Liss; 2002:19–56.
18. Kurita H, Yamamoto E, Nozaki S, Wada S, Furuta I, Kurashina K. Multicenter phase I trial of induction chemotherapy with docetaxel and nedaplatin for oral squamous cell carcinoma. *Oral Oncol.* 2004;40:1000–1006.
19. Fuwa N, Kodaira T, Kamata M, et al. Phase I study of combination chemotherapy with 5-fluorouracil (5-FU) and nedaplatin (NDP): adverse effects and recommended dose of NDP administered after 5-FU. *Am J Clin Oncol.* 2002; 25:565–569.
20. Suzuki S, Ishikawa K. Safety and efficacy of S-1 chemotherapy in recurrent/metastatic head and neck cancer. *J Infect Chemother.* 2009;15:335–339.
21. Machulla HJ, Blocher A, Kuntzsch M, Piert M, Wie R, Grierson JR. Simplified labeling approach for synthesizing 3′-deoxy-3′-[^{18}F]fluorothymidine ([^{18}F]FLT). *J Radioanal Nucl Chem.* 2000;243:843–846.
22. Toyohara J, Waki A, Takamatsu S, Yonekura Y, Magata Y, Fujibayashi Y. Basis of FLT as a cell proliferation marker: comparative uptake studies with [^{3}H]thymidine and [^{3}H]arabinothymidine, and cell-analysis in 22 asynchronously growing tumor cell lines. *Nucl Med Biol.* 2002;29:281–287.
23. Mankoff DA, Shields AF, Krohn KA. PET imaging of cellular proliferation. *Radiol Clin North Am.* 2005;43:153–167.
24. Sugiyama M, Sakahara H, Sato K, et al. Evaluation of 3′-deoxy-3′-^{18}F-fluorothymidine for monitoring tumor response to radiotherapy and photodynamic therapy in mice. *J Nucl Med.* 2004;45:1754–1758.
25. Yang YJ, Ryu JS, Kim SY, et al. Use of 3′-deoxy-3′-[^{18}F]fluorothymidine PET to monitor early responses to radiation therapy in murine SCCVII tumors. *Eur J Nucl Med Mol Imaging.* 2006;33:412–419.
26. Apisarnthanarax S, Alauddin MM, Mourtada F, et al. Early detection of chemoradioresponse in esophageal carcinoma by 3′-deoxy-3′-^{3}H-fluorothymidine using preclinical tumor models. *Clin Cancer Res.* 2006;12:4590–4597.
27. Menda Y, Boles Ponto LL, Dornfeld KJ, et al. Kinetic analysis of 3′-deoxy-3′-^{18}F-fluorothymidine ((^{18}F)-FLT) in head and neck cancer patients before and early after initiation of chemoradiation therapy. *J Nucl Med.* 2009;50:1028–1035.
28. Linecker A, Kermer C, Sulzbacher I, et al. Uptake of (^{18}F)-FLT and (^{18}F)-FDG in primary head and neck cancer correlates with survival. *Nuklearmedizin.* 2008; 47:80–85.
29. Andrade RS, Heron DE, Degirmenci B, et al. Posttreatment assessment of response using FDG-PET/CT for patients treated with definitive radiation therapy for head and neck cancers. *Int J Radiat Oncol Biol Phys.* 2006;65:1315–1322.
30. Porceddu SV, Jarmolowski E, Hicks RJ, et al. Utility of positron emission tomography for the detection of disease in residual neck nodes after (chemo) radiotherapy in head and neck cancer. *Head Neck.* 2005;27:175–181.
31. Schöder H, Fury M, Lee N, Kraus D. PET monitoring of therapy response in head and neck squamous cell carcinoma. *J Nucl Med.* 2009;50(suppl):74S–88S.
32. Ryan WR, Fee WE Jr, Le Q, Pinto HA. Positron-emission tomography for surveillance of head and neck cancer. *Laryngoscope.* 2005;115:645–650.
33. Quon A, Fischbein NJ, McDougall IR, et al. Clinical role of ^{18}F-FDG PET/CT in the management of squamous cell carcinoma of the head and neck and thyroid carcinoma. *J Nucl Med.* 2007(suppl);48:58S–67S.
34. Malone JP, Gerberi MA, Vasireddy S, et al. Early prediction of response to chemoradiotherapy for head and neck cancer: reliability of restaging with combined positron emission tomography and computed tomography. *Arch Otolaryngol Head Neck Surg.* 2009;135:1119–1125.
35. Goerres GW, Schmid DT, Bandhauer F, et al. Positron emission tomography in the early follow-up of advanced head and neck cancer. *Arch Otolaryngol Head Neck Surg.* 2004;130:105–109.
36. Hoshikawa H, Kishino T, Nishiyama Y, Yamamoto Y, Yonezaki M, Mori N. Early prediction of local control in head and neck cancer after chemoradiotherapy by FDG PET. *Nucl Med Commun.* 2011;32:684–689.
37. Everitt S, Hicks RJ, Ball D, et al. Imaging cellular proliferation during chemoradiotherapy: a pilot study of serial ^{18}F-FLT positron emission tomography/computed tomography imaging for non-small-cell lung cancer. *Int J Radiat Oncol Biol Phys.* 2009;75:1098–1104.